RESEARCH PAPER

Computational assessment of drug-induced effects on the electrocardiogram: from ion channel to body surface potentials

Nejib Zemzemi[1,2], Miguel O Bernabeu[1], Javier Saiz[3], Jonathan Cooper[1], Pras Pathmanathan[1], Gary R Mirams[1], Joe Pitt-Francis[1] and Blanca Rodriguez[1]

[1]Department of Computer Science, University of Oxford, Oxford, UK, [2]INRIA Bordeaux Sud-Ouest CARMEN project, Talence, France, and [3]Universidad Politécnica de Valencia, Valencia, Spain

BACKGROUND AND PURPOSE

Understanding drug effects on the heart is key to safety pharmacology assessment and anti-arrhythmic therapy development. Here our goal is to demonstrate the ability of computational models to simulate the effect of drug action on the electrical activity of the heart, at the level of the ion-channel, cell, heart and ECG body surface potential.

EXPERIMENTAL APPROACH

We use the state-of-the-art mathematical models governing the electrical activity of the heart. A drug model is introduced using an ion channel conductance block for the hERG and fast sodium channels, depending on the IC_{50} value and the drug dose. We simulate the ECG measurements at the body surface and compare biomarkers under different drug actions.

KEY RESULTS

Introducing a 50% hERG-channel current block results in 8% prolongation of the APD_{90} and 6% QT interval prolongation, hERG block does not affect the QRS interval. Introducing 50% fast sodium current block prolongs the QRS and the QT intervals by 12% and 5% respectively, and delays activation times, whereas APD_{90} is not affected.

CONCLUSIONS AND IMPLICATIONS

Both potassium and sodium blocks prolong the QT interval, but the underlying mechanism is different: for potassium it is due to APD prolongation; while for sodium it is due to a reduction of electrical wave velocity. This study shows the applicability of in silico models for the investigation of drug effects on the heart, from the ion channel to the ECG-based biomarkers.

Abbreviations

AP(D), action potential (duration); APD_{90}, the action potential duration at 90%; hERG, human ether-a-go-go related gene, encoding the major I_{Kr} channel protein; ICH, International Conference on Harmonisation of Technical Requirements for Registration of Pharmaceuticals for Human Use; IC_{50}, the half-maximal inhibitory concentration; I_{Kr}, rapidly activating potassium current; I_{Ks}, slowly activating potassium current; I_{Na}, fast sodium current; I_{CaL}, L-type calcium current; QT(c), the Q to T interval of the ECG (corrected for heart rate); V_m, transmembrane potential

Introduction

Even though drugs are designed to bind to specific targets to treat specific diseases, many of them exhibit multiple off-target interactions, which can lead to drug safety problems. Prediction of these undesirable drug-induced side effects is a major goal for pharmaceutical companies and regulatory agencies (Recanatini *et al.*, 2005). The total estimate of preclinical and clinical assessments for a compound that is released to the market is at least $800 million (see Adams and Brantner, 2006). Withdrawal of a drug after approval represents not just a safety risk to patients but also a massive loss of investment of resources, time and money. Predicting drug side effects in the heart as early as possible during the drug development process is therefore a priority for safety pharmacology (Pollard *et al.*, 2010).

One of the most dangerous potential drug side effects is electrophysiological cardiotoxicity (Valentin and Hammond, 2008), resulting from pro-arrhythmic abnormalities in the electrical activity of the heart caused by the interaction of drug molecules with cardiac ion channels. According to some estimates, around 40% of all novel pharmaceutical compounds have an effect on cardiac ion channels (Noble, 2008). In the worst-case scenario, drug side effects can result in sudden cardiac death caused by lethal arrhythmias such as Torsades de Pointes (see Krikler and Curry, 1976 and De Bruin *et al.*, 2005).

Since arrhythmias are rarely observed in clinical trials, a variety of both preclinical and clinical biomarkers have been proposed to predict drug-induced pro-arrhythmic risk in several animal models as well as humans (Corrias *et al.*, 2010). The QT interval in the ECG is one of the main biomarkers used in the assessment of cardiac safety (Recanatini *et al.*, 2005; Pollard *et al.*, 2010). Quantification of drug-induced effects on the QT interval is mandatory in the clinical human Thorough QT trial (Gintant, 2011) before approval by regulatory agencies, following the *Guidance for Industry* report (ICH. E14, 2005). Drugs that prolong or shorten the QT interval in the ECG are considered to have pro-arrhythmic consequences (Straus *et al.*, 2005; Kowey and Malik, 2007; Lu *et al.*, 2008; Pugsley *et al.*, 2008), and their development is generally discontinued.

Preclinical assessment of cardiac compounds therefore aims at detecting drugs that would result in QT prolongation in the clinical Thorough QT trial. Different testing strategies (Pugsley *et al.*, 2008) are applied to assess drug cardiac safety, including:

(i) ion channel binding assays (to determine the binding affinity between the drug and cardiac ion channels);
(ii) voltage-clamp analysis of ion-channel currents (in particular the hERG potassium channel; see (Curran *et al.*, 1995; Vandenberg *et al.*, 2001; Redfern *et al.*, 2003; Sanguinetti and Mitcheson, 2005; Hancox *et al.*, 2008; Gintant, 2011);
(iii) action potential recordings in isolated myocytes and tissue (see Hondeghem *et al.*, 2001; Valentin *et al.*, 2004);
(iv) measurement of drug-induced changes to the QT interval in small, and later large, mammals (Fossa *et al.*, 2002).

However, predicting drug-induced QT prolongation in the Thorough QT trial from the results of preclinical testing presents some unresolved issues, related to the fact that preclinical assessment heavily relies on animal testing. This implies ethical concerns, which trigger the need for the development of novel methodologies to reduce, refine and replace animal experimentation. Interspecies differences in drug effects between animals and humans could also explain limitations in the predictive capacity of preclinical models, as quantified in previous studies (Valentin and Hammond, 2008).

In recent years, computational modelling and simulation has proven to be a powerful tool for investigations of the effect of drugs, mutations and disease on cardiac electrophysiological activity (Clancy and Rudy, 1999; Sale *et al.*, 2008). The sophistication of current computational physiology technology and its application to drug safety assessment has attracted the interest of both regulatory agencies and industry, as shown in recent papers (Davies *et al.*, 2012; Fletcher *et al.*, 2011; Mirams *et al.*, 2011; Valentin and Hammond, 2008; Soubert *et al.*, 2009; Sanchez *et al.*, 2012). In the present study, we describe the first computer simulations of the effect of drug action on the electrophysiological activity of the human ventricles from the ion channel to the body surface potentials. A three-dimensional human whole-body model with biophysically detailed representation of electrophysiological ionic processes in the heart is developed based on human anatomical and functional data. Computer simulations are conducted using the human body model to investigate the multiscale effects of potassium and sodium blockers on ionic currents, on action potential throughout the ventricles, on whole-ventricular activation and repolarization dynamics and on body surface potentials.

Methods

In this section, we provide a description of the models, numerical algorithms, computational software and the anatomical model used to simulate the electrical propagation from cardiac ionic currents to body surface.

Three-dimensional (3D) anatomical model of the human body

A 3D anatomical finite-element mesh of the human body was developed from human anatomical data[1] as described in Chapelle *et al.* (2009). Figure 1A presents the computational mesh including a detailed representation of the heart and surrounding tissues such as bones and lungs. In brief, data were pre-processed using the 3-matic[2] software in order to obtain surface meshes, and then the meshing software Yams (Frey, 2001) and GHS3D (George *et al.*, 1990) to further process the surface meshes and generate the final 3D computational meshes. The mesh contains 2 401 151 vertices and 14 336 528 tetrahedral elements. The resolution of the mesh in the heart is 0.06 cm, close to the value of 0.05 cm reported as sufficient to ensure numerical convergence in terms of

[1]http://www.3dscience.com
[2]http://www.materialise.com

A

B

C
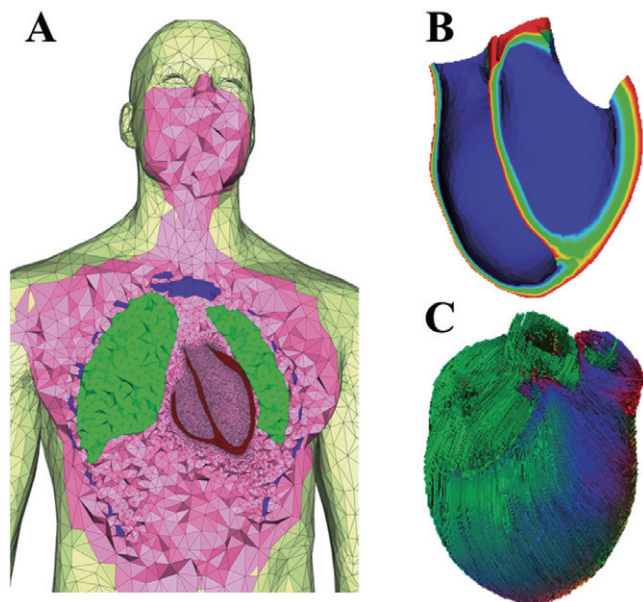
Figure 1

A. Human body mesh including detailed representation of the cardiac ventricles as well as lung, skeleton and remaining tissue. B. Definition of cell heterogeneity in the human cardiac ventricles including endocardium, mid-myocardium and epicardium. C. Orientation of ventricular fibres in the human ventricular model. These meshes were generated and processed in collaboration with INRIA[3] (Chapelle *et al.*, 2009).

conduction velocity and activation times using the Chaste software (see Niederer *et al.*, 2011).

In order to introduce anisotropy in the myocardium, realistic fibre orientation was included in the model using a rule based method (Bishop *et al.*, 2009), as shown in Figure 1C.

Electrical model

The electrical activity throughout the ventricles and the whole body is simulated using the bidomain equations and the human mesh described above. In brief, the bidomain model represents the myocardium as two domains, the intracellular and extracellular domains, connected by the cell membrane, at each mesh point (see, e.g. Tung, 1978; Sundnes *et al.*, 2006). The Laplace equation is used to compute extracellular potentials in the human body, outside the heart. The equations are used to calculate at each time the distribution of transmembrane potentials at each point in the heart and the distribution of the extracellular potential at each point of the body.

In our model, the heart–torso interface is assumed to be a perfect conductor, allowing for continuity of both current and potential between the extracellular myocardial region and the torso region. Previous studies (Lines *et al.*, 2003a; Potse *et al.*, 2003; Clements *et al.*, 2004) consider heart and torso to be isolated; that is, the electrical current does not flow from the heart to the torso. This approximation reduces computational cost because it uncouples the Laplace equa-

[3]http://www.inria.fr/en/

tion in the torso from the bidomain equations in the heart, but numerical evidence has shown that it can compromise the accuracy of the ECG signals (see, e.g. Lines *et al.*, 2003b; Pullan *et al.*, 2005; Boulakia *et al.*, 2010). Thus, in order to compute ECGs accurately, we consider the state-of-the-art heart–torso fully coupled electrophysiological problem representing the cardiac electrical activity from the cell to the human body surface. Details on the model equations can be found in the Supporting Information Appendix S1 (section 'Electrical Model').

Heterogeneity in conductivities in the heart and different parts of the body highlighted in Figure 1A was represented in the model by considering different conductivity tensor values. The conductivity tensor in the torso was assumed isotropic. The torso conductivity σ_T depends on three different regions defined in the computational mesh: $\sigma_T = 0.056$ S cm^{-1} in the skeleton (Schwan and Kay, 1957), $\sigma_T = 0.9$ S cm^{-1} in the lung (Rush and Driscoll, 1969), and $\sigma_T = 0.76$ S cm^{-1} in the transverse skeletal muscle conductivity (Epstein and Foster, 1983), for the remaining tissue. Conductivities in the myocardium were taken from Clerc (1976).

In the absence of the Purkinje network, a time-dependent initial stimulus was applied on the endocardium to mimic a realistic electrical activation sequence in the heart. Propagation of the electrical excitation throughout the ventricles occurred from apex to base following endocardial stimulation in the left and the right ventricle. The duration of the intra-cellular stimulus was 0.5 ms, and its strength was 100 mA cm^{-3}.

Human ventricular action potential model including drug action

Membrane kinetics at each human ventricular mesh point was represented by the biophysically detailed TP06 human ventricular action potential model (Ten Tusscher and Panfilov, 2006). In brief, the TP06 model includes equations for the main ion channels, transporters and pumps involved in the generation of the human action potential and the associated intracellular sodium, calcium and potassium concentrations. Calcium dynamics in the subspace, cytoplasm and sarcoplasmic reticulum are also represented in the model. The Ten Tusscher and Panfilov model has been extensively used and compared against experimental human data, showing good performance in terms of action potential and repolarization mechanisms (Romero *et al.*, 2009). It therefore represents an adequate model to investigate drug-induced effects on repolarization mechanisms from multiple drug/ion channel interaction to surface body ECG. Transmural heterogeneity in ionic properties was also included as in previous studies (Ten Tuscher and Panfilov, 2006). Whereas the causes of and gradients in transmural heterogeneity are under debate and have been reported to take many forms (Yan *et al.*, 2003; Glukhov *et al.*, 2010; Keller *et al.*, 2011; Janse *et al.*, 2012), here we chose to represent three layers, corresponding to epicardial, midmyocardial and endocardial tissue, by assigning specific properties to the transient outward current (Ito), and the slow and rapid components of the delayed rectifier potassium current (IKs and IKr), similar to Ten Tusscher and Panfilov (2006).

The human TP06 action potential model was modified to include the action of potassium and sodium blockers. A

single pore block model was used (similar to Brennan *et al.*, 2009; Mirams *et al.*, 2011; Zemzemi *et al.*, 2011) to model the drug-ionic current response curve (i.e. the amount of current block with respect to drug dose, based on the drug IC_{50} value and a Hill coefficient). In this study, we simulated the effect of blocking I_{Kr} using two concentrations equal to IC_{50} and 10 times IC_{50} values and the effect of blocking the fast Na current I_{Na} using IC_{50} value and twice IC_{50} value. These drug doses are in the range of the doses prescribed clinically, which are usually less than 30 times the IC_{50} value (see Redfern *et al.*, 2003; Mirams *et al.*, 2011). The model could be easily extended to include drug effects on multiple ionic currents by modifying the corresponding ionic conductances as done here for the potassium and the sodium currents. We also considered two different I_{CaL} conductances to explore how reported gender differences in I_{CaL} (Verkerk *et al.*, 2005; Grandy and Howlett, 2006; Sims *et al.*, 2008) could have a potential impact in drug induced changed in the ECG. Simulations were conducted for two values of L-type calcium current (I_{CaL}) conductance corresponding to its control value in the TP06 model (male) and an increased value by 30% with respect to control (female) (Verkerk *et al.*, 2005).

Numerical implementation

All the simulations presented in this study were run with the open source software package Chaste (Pitt-Francis *et al.*, 2009). Chaste (Cancer, Heart and Soft Tissue Environment) provides an integrated modelling and simulation environment for a wide range of Systems Biology problems. The software can be downloaded from http://www.cs.ox.ac.uk/chaste. The Chaste bidomain finite element solver has been used for a number of simulation studies (see, for instance, Corrias *et al.*, 2010), but this was the first time Chaste was used to simulate the electrical activity of the heart embedded in a human body mesh for ECG simulation.

Equations (1) to (3) (in the Supporting Information Appendix S1) are solved by means of a semi-implicit time discretization, where the diffusion term is treated implicitly and the reaction term semi-implicitly (i.e. the transmembrane potential V_m is treated explicitly in the ODE system, while the time derivative is approximated implicitly). For the space discretization, a finite element method with tetrahedral elements and piecewise linear basis functions was chosen.

The reader can refer to Pathmanathan *et al.* (2010) for a detailed discussion on Chaste's numerical methods. Chaste's parallelization is based on the message-passing standard Message Passing Interface (MPI), and it uses ParMETIS to ensure optimal domain decomposition. A shared-memory aware MPI implementation was used to improve intra-node communications.

Chaste uses PyCML (Cooper, 2009) to generate optimized C++ code on the fly from any valid CellML file describing a cardiac ionic model, like the Ten Tusscher and Panfilov (2006) model used in this work. Chaste also includes the capability of automatically generating realistic fibre orientation and heterogeneities in ionic properties in anatomically based geometrical models (Bernabeu *et al.*, 2008). The simulations were conducted on the HECToR[4] supercomputer using 2048 cores

[4]http://www.hector.ac.uk

distributed on 128 nodes; each node has 32GB of memory. A simulation of a heart beat takes 1.5 h.

Data analysis

The ECG was computed according to the standard 12-lead ECG definition (see Malmivuo and Plonsey, 1995 for instance). This includes the Einthoven limb leads (I, II and III), the augmented leads (aVR, aVL, aVF) as well as the six precordial leads (V1–V6).

The analysis of the simulation results also included the generation of activation and repolarization maps, which depict the time of activation and repolarization for each point in the human ventricular mesh respectively. Local activation time for each point was computed as the time at which the transmembrane potential reaches –30 mV. Local repolarization time at each ventricular mesh point was computed as the time at which the transmembrane potential reached 90% of repolarization. The APD_{90} at each mesh point was computed as the difference between the activation and the repolarization time. The dispersion of transmembrane potential is computed as the difference between the maximum and the minimum values of V_m in the heart at each time step. The analysis is also based on the QT and QRS durations, the T_{peak}–T_{end} interval and the amplitude of the T wave in the ECG.

Results

Simulation of the human ECG under normal conditions

Figure 2 describes the simulation results using the human heart–torso coupled model described above for control conditions. Figure 2A and B show the ECG recorded in lead I and the distribution of body potentials during the activation and the repolarization phase, recorded at 40 and 310 ms after the endocardial stimulation respectively. Figure 2C shows an endocardial view of the activation maps, illustrating the propagation of the electrical excitation from apex to base and from endocardium to epicardium. The total activation time is 76 ms, which is the time taken by the wave to propagate to the epicardium at the base of the ventricles. Figure 2D shows a basal view of the repolarization map of the human ventricles under control conditions. Results indicate that the longest repolarization times of 363 ms are those of tissue in the mid-myocardium of the ventricular base.

Figure 3 presents the ECG recorded in the 12 leads obtained from the human body simulations under control conditions. Results show that the magnitude, duration and polarity of QRS and T-wave complexes in most of the leads are within physiological ranges (see, e.g. Malmivuo and Plonsey, 1995; Aehlert, 2006). Furthermore, the QRS complex duration is 76 ms and the QRS orientation changes between V3 and V4, indicating that the activation sequence in the normal ventricles is correctly reproduced (Aehlert, 2006).

The amplitude of the QRS in the lead II is very low. This seems to be a left axis deviation, possibly due to the initial activation. The QT duration in the simulated ECG under control conditions is 365 ms, which is within the physiological range of QT between 363 and 421 ms reported for 1 Hz
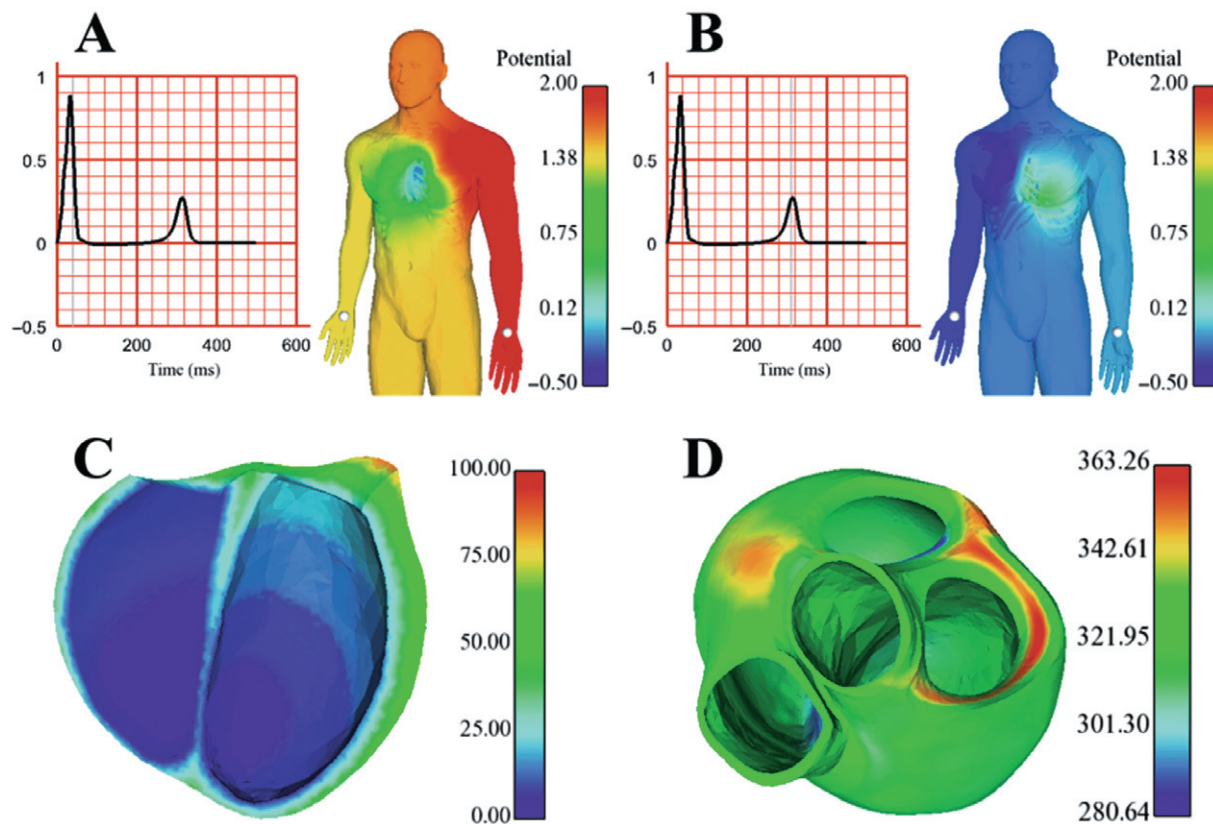
Figure 2

Top: Distribution of electrical potentials in the body surface in control conditions, during the activation phase (A, 40 ms following endocardial stimulation) and during the repolarization phase (B, 310 ms following endocardial stimulation). Lead I ECG plots in panels A and B are the difference between potentials recorded in the left and the right arms (in the white ball locations). The colour bar provides a colour distribution of the potential in mV. Panels C and D show an endocardial view of the activation time maps and a basal view of the repolarization time maps in the human ventricles respectively.

stimulation frequency (see Karjalainen *et al.*, 1994; Malik *et al.*, 2002). Although in the precordial leads the T wave seems to have the right amplitude, in the three limb leads (I, II, III) and the augmented leads (aVF, aVL and aVR), the T-wave amplitude is low.

Simulation of the effect of potassium channel block on the ECGs

The interaction of drug action with the hERG channel is a major concern for pharmaceutical companies as it is thought to result in QT prolongation and increased risk of lethal arrhythmias. Using the human torso model described above, we simulated the effect of a potassium channel blocker on the electrical activity of the ventricles and on the ECG, for two drug doses equal to IC_{50} and 10 times IC_{50} concentrations. As explained above, simulations were conducted for two different values of the I_{CaL} conductance, the control TP06 value and an increased conductance by 30% from control. The simulations allowed an investigation into the role of I_{CaL} conductance in modulating the action of hERG channel block on ventricular activity and ECG.

As expected, Figure 4 shows that hERG block results in QT prolongation and changes in the T wave in the 12 leads of the

simulated ECG. As shown in Figure 5A for the lead I ECG, the effects of hERG block on the ECG are dose-dependent and result in prolongation of the QT interval from 365 ms in control to 386 ms and 405 ms for IC_{50} and 10 times IC_{50} drug dose, and in reduction of T-wave amplitude from 0.27 mV in control to 0.2 mV for IC_{50} and 0.14 mV for 10 times IC_{50} drug dose. Changes in the ECG following hERG block administration are explained by the effect of the drug on the action potential and repolarization time maps, as shown in Figure 5C. Although the pattern of repolarization time distribution is similar for all doses (Figure 5C), the magnitude of the repolarization times is modified (see colour bar scales in Figure 5C), due to a prolongation of the action potential duration at each location of the heart. This can be seen in Figure 5B where we show the action potential traces recorded at a specific location at the base of the ventricles for the three drug doses considered. As shown in this figure, activation time is not affected by drug application, but APD however is clearly prolonged from 282 ms in control to 304 and 324 ms for IC_{50} and 10 times IC_{50} drug dose, respectively (thus by 7.8% and 15% respectively). APD prolongation results in delayed repolarization times and QT prolongation but by a smaller amount (by 5.7% and 11% respectively). This differ-
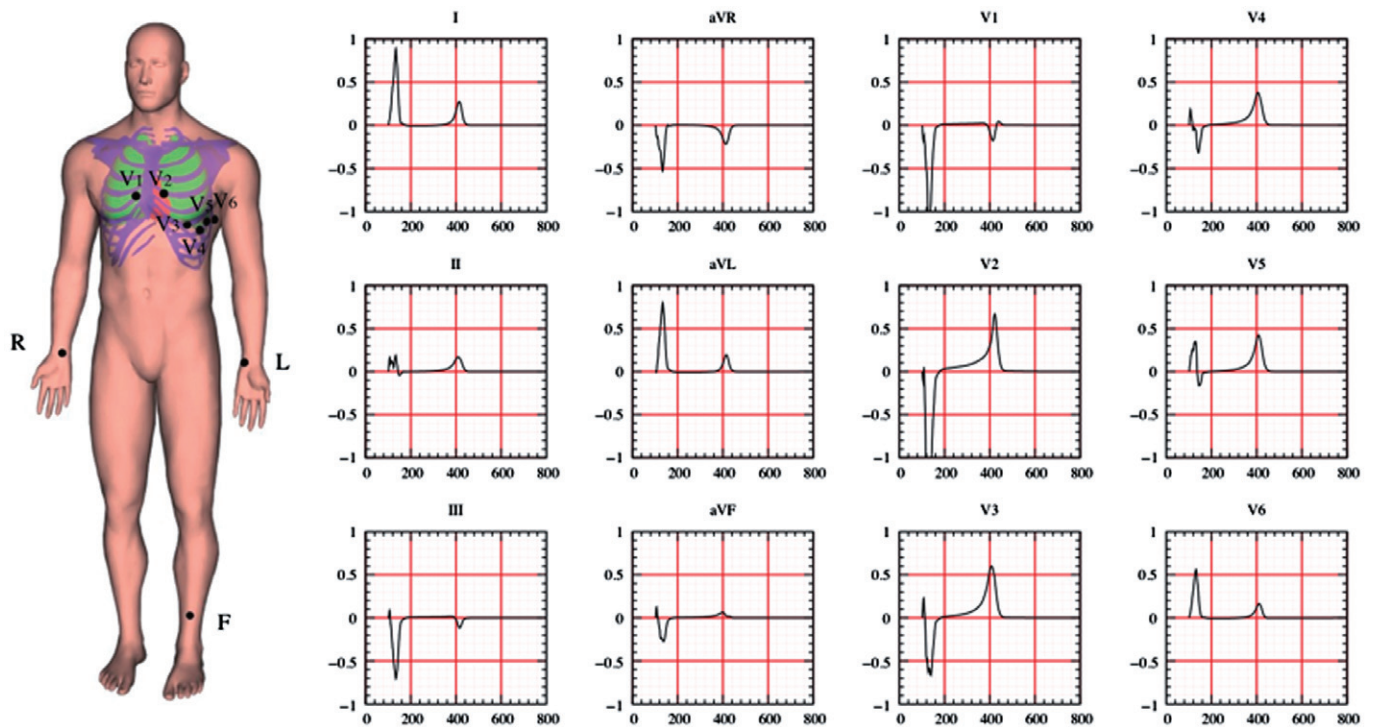
Figure 3
Simulated standard 12-lead ECG (right) using the human torso model and the 9-lead positions (left) in normal conditions: *X*-axis (small square, 40 ms; big square, 200 ms), *Y*-axis (small square, 0.1 mV; big square, 0.5 mV) (right).

ence between the percentage of increasing the APD_{90} and the QT interval shows that performing a single-cell study of the drug effect is not enough to predict the percentage of QT prolongation. Furthermore, Figure 5B shows that increasing drug dose reduces the slope of the action potential during the repolarization phase, which could also explain the decrease in T-wave magnitude. Importantly, our simulations highlight the lack of 1/1 ratio in the relationship between QT and T wave and hERG block, caused by the highly nonlinear dynamics determined by both structural and functional factors underlying cardiac electrophysiology taken into account in our model.

Figure 6 provides further quantification of drug-induced changes in biomarkers extracted from the simulations including the QT interval, the maximum repolarization time in the ventricles, the QRS complex duration, T_{peak}–T_{end} duration, T-wave amplitude and the maximum dispersion of transmembrane potentials in the ventricles during the repolarization phase. Figure 6A–C corresponds to control I_{CaL} simulations, whereas Figure 6D–F shows results for increased I_{CaL}.

As shown in Figures 4 and 5, hERG block results in the dose-dependent prolongation of the QT interval, which is a reflection of the drug-induced increase in repolarization times. hERG block however does not affect the QRS interval and the T_{peak}–T_{end} duration (Figure 6B and E). In contrast, the T-wave amplitude and the maximum V_m dispersion are reduced during the repolarization phase, also in a dose-dependent manner (Figure 6C and F); therefore, the reduction is larger for the larger applied drug dose.

As shown in Figure 6, the drug-induced changes are qualitatively similar for both I_{CaL} conductance values considered (compare top and bottom panels). However, increase in I_{CaL} conductance results in: (i) prolongation of QT interval duration, maximum repolarization time and T_{peak}–T_{end} interval duration; (ii) slight decrease in QRS duration; (iii) increase in T-wave amplitude and in maximum V_m dispersion, as shown in Figure 6. The changes in the ECG caused by increased I_{CaL} levels are due to an increase in the duration and plateau V_m levels as shown in Figure 7.

Simulation of the effect of sodium channel block on the ECGs

The sodium channel, also known as SCN5A-encoded Na^+ channel, is the main contributor to the activation of the myocardial cell (see Kohlhardt *et al.*, 1972). The fast sodium channels are responsible for the rapid depolarization of the cell (AP phase 0), playing an important role in determining the action potential upstroke velocity at a cell level (Salata and Wasserstrom, 1988) as well as the propagation velocity in tissue (Bezzina *et al.*, 2006; Lu *et al.*, 2010). The drugs that mainly target the sodium channels are known as class I drugs. They are used to treat different atrial and ventricular arrhythmia like tachycardia and fibrillation, but they can increase arrhythmic risk (see Yap and Camm, 2003).

Figure 8 illustrates the simulated first ECG-lead (A), the action potential traces at a basal ventricular location (B) as well as activation (C) and repolarization (D) maps for control, IC_{50} and twice IC_{50} doses of a sodium blocker. Quantification of biomarkers is also shown in the histograms presented in
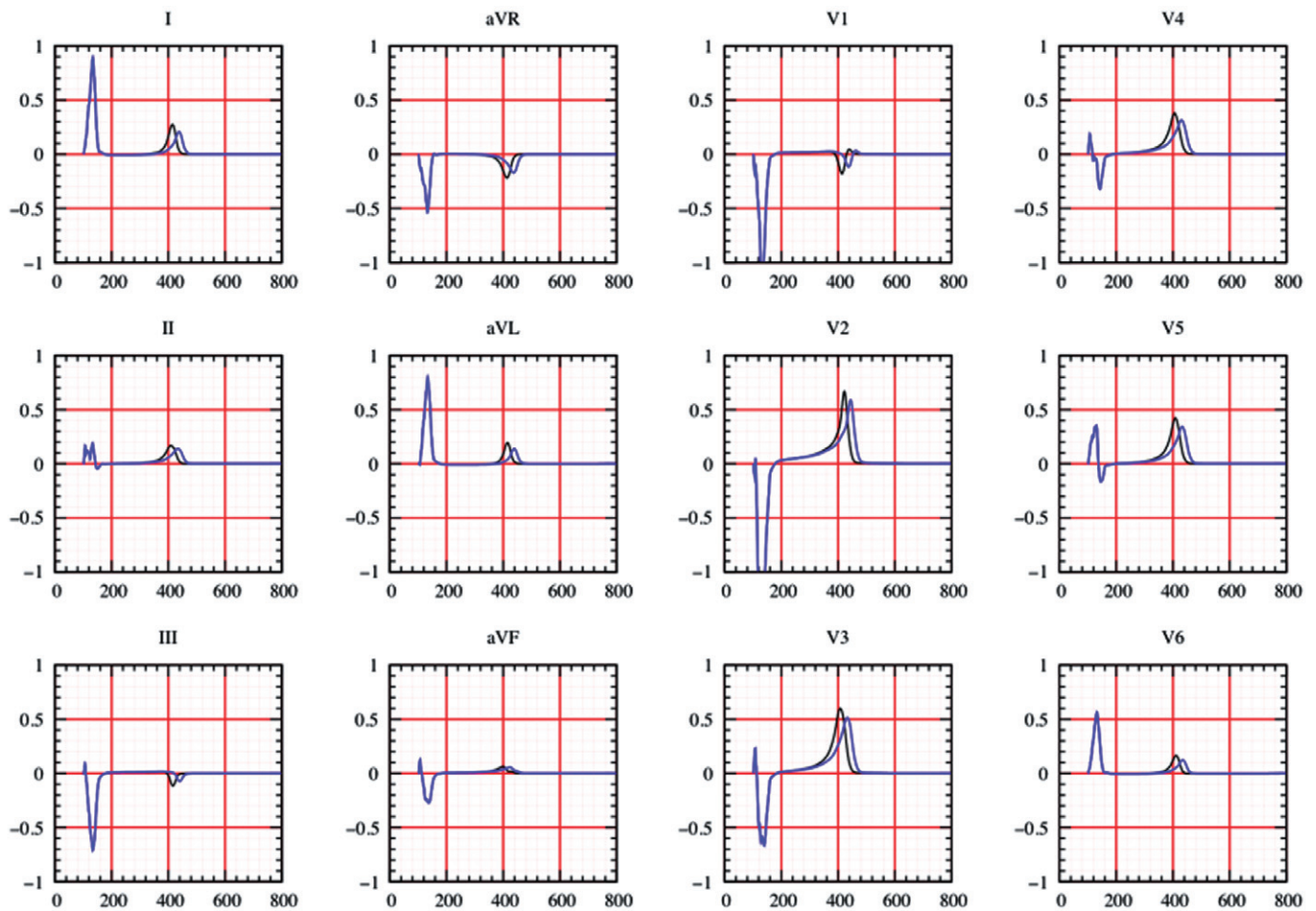
Figure 4

Effect of hERG channel block on the simulated 12-lead ECG. Body surface potentials recorded for the 12-lead ECG are shown for normal conditions and following application of an IC_{50} dose of a hERG channel blocker: X-axis (small square, 40 ms; big square, 200 ms), Y-axis (small square, 0.1 mV; big square, 0.5 mV).

Figure 9. Figure 9 provides further quantification for the drug-induced changes in different biomarkers obtained from the simulations. Figure 9A and C corresponds to control I_{CaL} simulations, whereas Figure 9D and F shows results for increased I_{CaL}. The results of the simulations presented in Figures 8 and 9 show that sodium block results in (i) the prolongation of QT interval, delayed activation time and increase in QRS interval; (ii) negligible effect on the $T_{peak}–T_{end}$ interval; (iii) decrease in T-wave amplitude and (iv) increase in maximum V_m dispersion.

The simulated ECG traces show that sodium block causes an enlargement of the QRS interval of about 18 and 30 ms for IC_{50} and twice IC_{50} drug doses (Figures 8A and 9A). This is caused by the delay in activation times (Figure 8C), resulting from a decrease in conduction velocity throughout the ventricles due to slow upstroke velocity of the action potential (Figure 8B).

Even though sodium channel block does not affect the repolarization phase of the action potential at the cell level (see Figure 8D, showing the APD_{90} distribution), the T wave

in the ECG exhibits important changes in polarity and amplitude (Figure 8A). The deflection of the T wave could be explained by a change of the repolarization wave polarity introduced by a long delay in the activation in the base of the heart. The decrease in the magnitude of the T wave is known to result from a reduction in the dispersion of repolarization, which may have important anti-arrhythmic consequences for the prevention of Torsades de Pointes in LQT2 and LQT3 models of the long-QT syndrome as mentioned in Shimizu and Antzelevitch (1997).

The changes in the ECG biomarkers are qualitatively similar for both I_{CaL} values considered (Figure 9). However, simulations show that increasing I_{CaL} by 30% results in QT prolongation and an increase in the T-wave amplitude for all the considered Na block doses. These changes are explained by the increase in plateau level and duration of the action potential illustrated in Figure 7A. However, maximum activation times, QRS, $T_{peak}–T_{end}$ and maximum V_m dispersion remained similar for both I_{CaL} values considered and all drug doses.
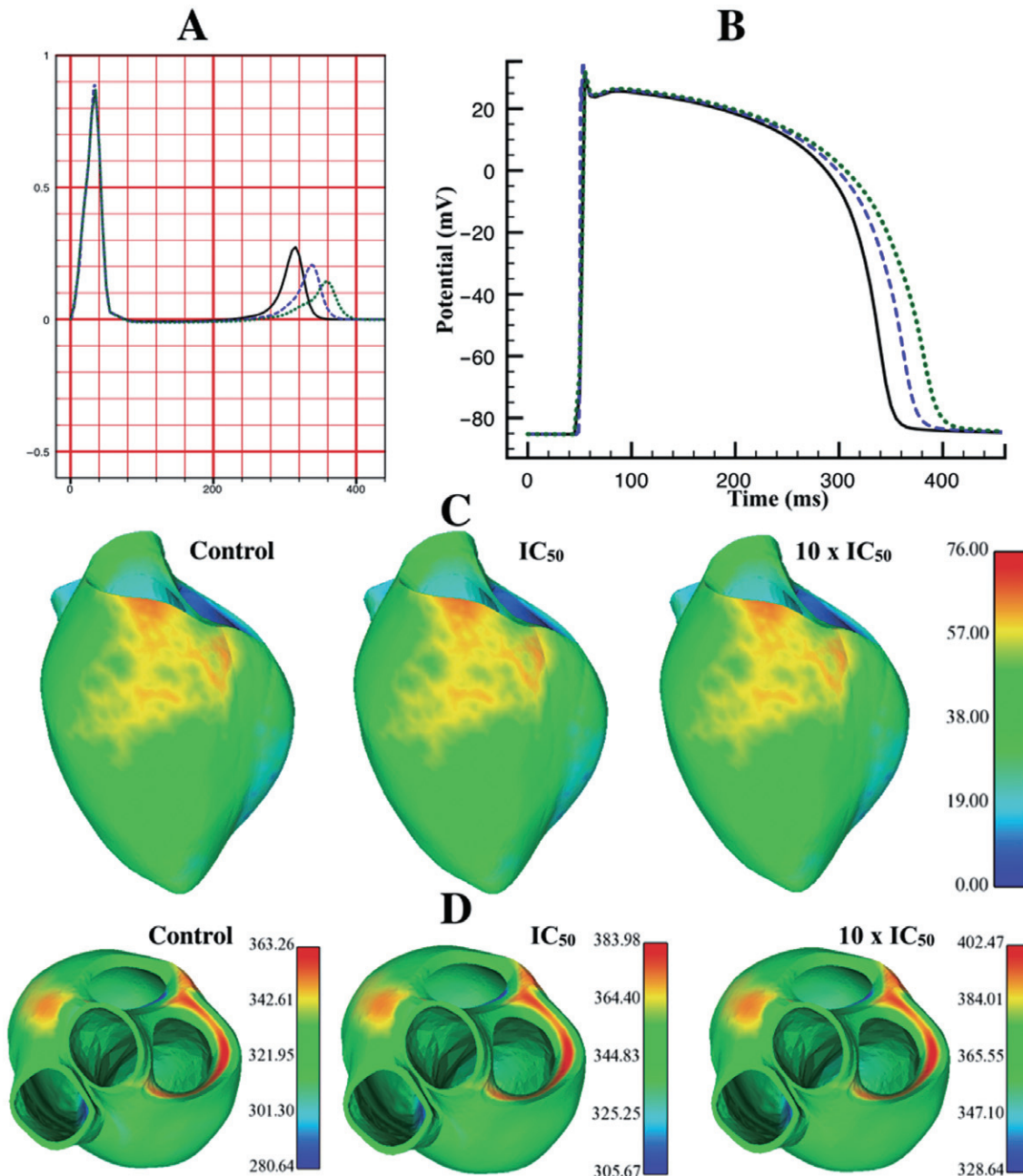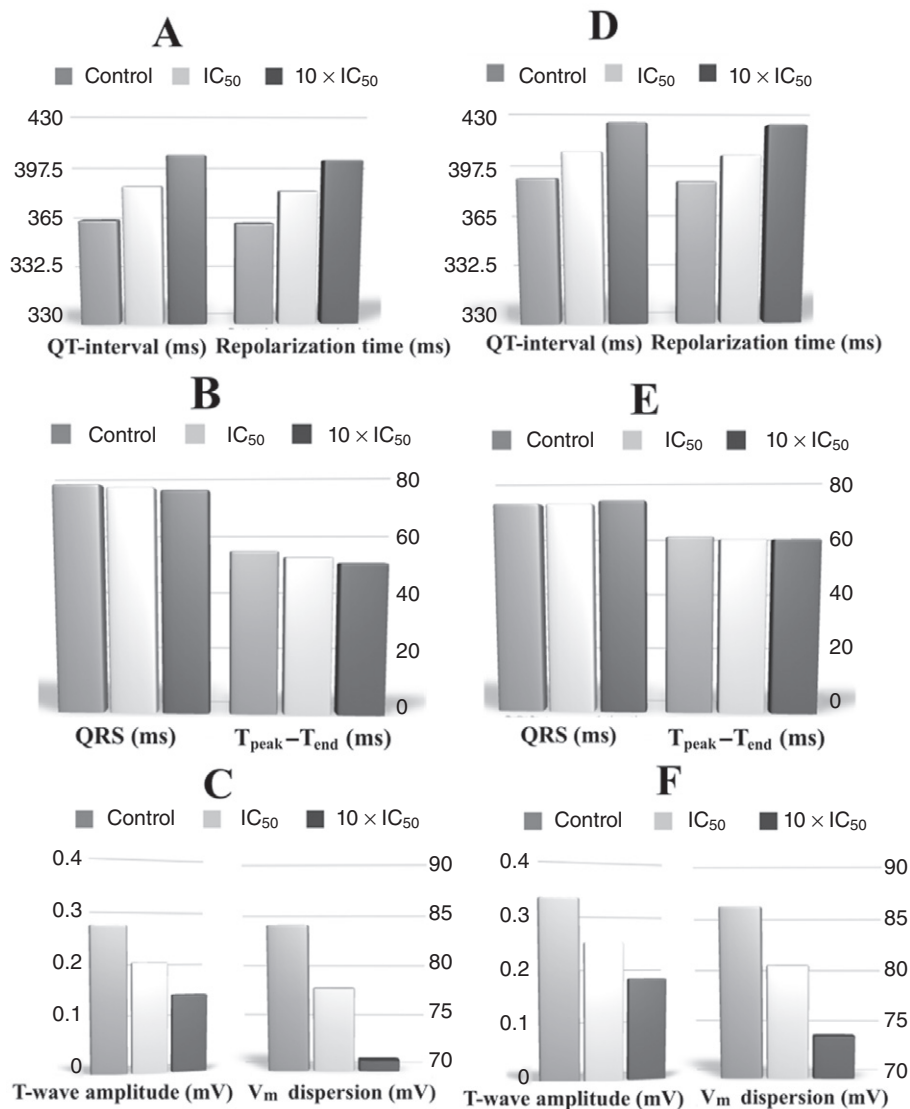
Figure 5

Simulated effect of hERG block on the lead I ECG(A) and time course of the action potential at a location of the base of the ventricles (B) for normal conditions, IC_{50} dose and 10 times the IC_{50} dose. Panel A, X-axis (small square, 40 ms; big square, 200 ms), Y-axis (small square, 0.1 mV; big square, 0.5 mV). Panel C (resp. D): left ventricle wall view of the activation (resp. repolarization) time maps for control, IC_{50} dose and 10 times IC_{50} from (left to the right). Times are in ms.

Discussion

The present study shows the first computer simulations of drug action from the ionic currents in the ventricles to the body surface electrocardiogram. A 3D multiscale human body anatomical model is constructed to simulate the clinical ECG, including the cardiac ventricles, lungs, bones and the surrounding tissue. The anatomically based electrophysiological model of the cardiac ventricles coupled to the whole body includes realistic representation of the ionic membrane kinetics, geometry, fibre orientation and electrophysiological heterogeneity in the ventricles. Computer simulations using the 3D human torso model and the efficient open source simulator Chaste are conducted under physiological conditions and following the application of sodium and potassium blockers, for several conductance values of the L-type calcium
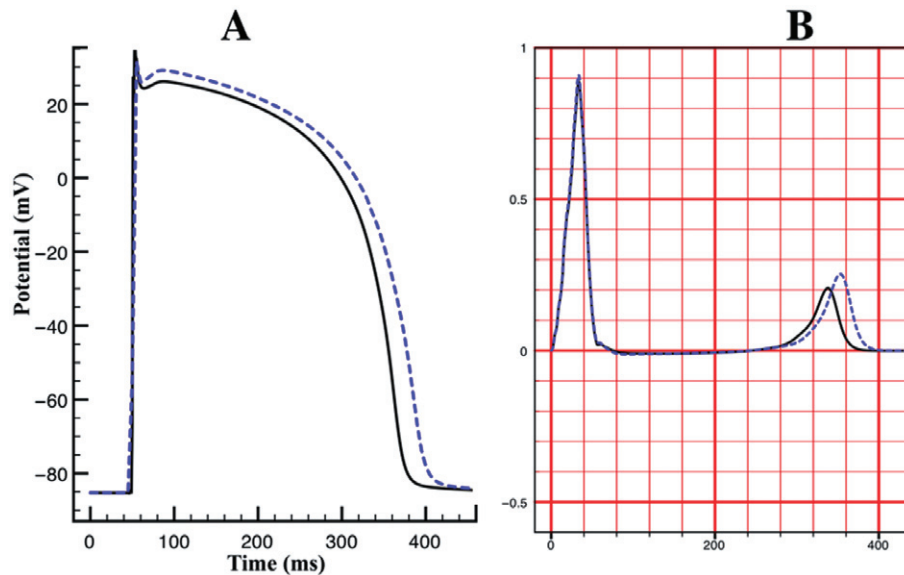
Figure 6

Histograms comparing the effect of a potassium blocker on different biomarkers for control condition IC$_{50}$ dose and 10 times IC$_{50}$ dose, when the L-type calcium current level is 100% (A, B and C) and when L-type calcium current level is 130% (D, E and F). Panel A (resp. D) compares the QT-interval and repolarization times for the three drug doses when the L-type calcium current level is 100% (resp. 130%). Panel B (resp. E) compares the QRS duration and the T$_{peak}$–T$_{end}$ when the L-type calcium current level is 100% (resp. 130%). Panel C (resp. F) compares T-wave amplitude and AP dispersion when the L-type calcium current level is 100% (resp. 130%).

current. Our study shows the power of multiscale simulations in bridging ionic, cellular, whole ventricular and body surface levels in cardiac electrophysiology to identify the nonlinear mechanisms underlying changes in ECG-based biomarkers caused by drug effects.

In agreement with clinical findings, simulation results show that the application of a potassium channel blocker results in QT interval prolongation as well as reduction in T-wave amplitude. As expected, QT interval prolongation is explained by APD prolongation caused by hERG block, whereas a decrease in T-wave amplitude correlates with a decreased dispersion in repolarization. The sodium channel block provokes a widening of QRS interval and QT interval prolongation in the ECG, caused by a prolongation of total

activation time due to decreased conduction velocity, in agreement with previous studies (Salata and Wasserstrom, 1988; Bezzina *et al.*, 2006). Therefore, our computer simulations are able to reproduce the known effects of potassium and sodium blockers on the electrophysiological activity of the ventricles at the ionic, cellular, whole ventricular and ECG levels. This could be considered as a first step towards the validation of electrophysiological model and the use of computational tools in drug effects assessment based on the ECG simulation. Simulations under physiological conditions and following sodium and potassium drug block were conducted for two values of the L-type calcium conductance (normal and increased by 30%). Variability in ionic currents, and in particular in the L-type calcium current, is thought to

Figure 7

Simulation of the effect of L-type calcium current level under potassium ion channel block. (A) Action potential trace when the potassium channel is half blocked and the L-type calcium level at 100% (respectively 130%). (B) Lead I ECG when the potassium channel is half blocked and 100% (130%, respectively) of L-type calcium level. *X*-axis (small square, 40 ms; big square, 200 ms), *Y*-axis (small square, 0.1 mV; big square, 0.5 mV).

underlie inter-subject and gender differences in pro-arrhythmic risk and ECG changes caused by pharmacological interventions (Romero *et al.*, 2009). Indeed, a large I_{CaL} conductance represents a large influx of calcium during the action potential and therefore an increased propensity for the development of early and delayed after-depolarizations (Miura *et al.*, 1993; Volders *et al.*, 2000). Large I_{CaL} conductance has also been suggested as one of the reasons for the higher propensity of development of drug-induced Torsades de Pointes in women than in men (Abi-Gerges *et al.*, 2004; Verkerk *et al.*, 2005). Our simulations show that increased I_{CaL} conductance results in slight decrease in QRS, prolongation of QT interval and increase in T-wave amplitude. At the cellular level, our simulations show that the changes are caused by increased conduction velocity due to a faster AP upstroke velocity and an increase in duration and amplitude of the plateau phase of the action potential.

Our study highlights the importance of 3D human body simulations for the prediction of the magnitude of drug-induced changes in the QT interval. In fact, when introducing a 50% potassium block, the percentage of APD_{90} prolongation was 7.8%, whereas the percentage of the QT interval prolongation was 5.7%, highlighting the nonlinear relationship between current block and changes in the ECG biomarkers. The difference between APD and QT prolongation is even larger for sodium channel blockers: the APD is not affected following application of IC_{50} or twice IC_{50} sodium block drug doses whereas the QT was prolonged by 5% for IC_{50} sodium block value and by 8.2% for twice the IC_{50} value. This highlights the need to consider the wide spatio-temporal dimensions required for the assessment of drug action on the heart and therefore the importance of using 3D human body models to predict drug effects on the ECG.

Previous studies have investigated the ionic mechanisms underlying changes in the ECG caused by mutations and diseased conditions. Most of the studies were conducted using the simulation of unipolar pseudo-ECGs using 1D or 3D anatomically based models (see, e.g. Gima and Rudy, 2002; Corrias *et al.*, 2010; Pueyo *et al.*, 2010; Dux-Santoy *et al.*, 2011). ECG simulations have also been performed using 3D heart models embedded in a torso (Lines *et al.*, 2003b; Chapelle *et al.*, 2009; Potse *et al.*, 2009; Zemzemi, 2009; Boulakia *et al.*, 2010; Keller *et al.*, 2011; Zemzemi *et al.*, 2011). The studies have shown the importance of torso effects in the simulation of the ECG. But they often included simplified or non-human ionic models or the obtained results are not in physiological ranges. The present study is however the first one to show the effect of drug action on the ECG using a biophysically detailed model of the cardiac ventricles embedded in a human torso model.

In our study, drug action at the ion channel level was simulated using a single pore block model, as in previous studies (Brennan *et al.*, 2009; Davies *et al.*, 2012; Mirams *et al.*, 2011). Although more sophisticated models of drug action have been developed (Clancy and Rudy, 2001; Moreno *et al.*, 2011; Saiz *et al.*, 2011), the single pore block model successfully reproduced the drug-induced decrease in conductance required. More sophisticated models of drug ion channel interaction, including multichannel effects, may be needed to simulate frequency-dependent effects, which were outside the scope of the study. Our approach also has the important advantage of using the output of high throughput ion channel assays, which is crucial in using the 3D model for preclinical drug safety testing in the pharmaceutical industry.

Simulations of specific ion channel blockers acting on the potassium or the sodium channels were considered, in order
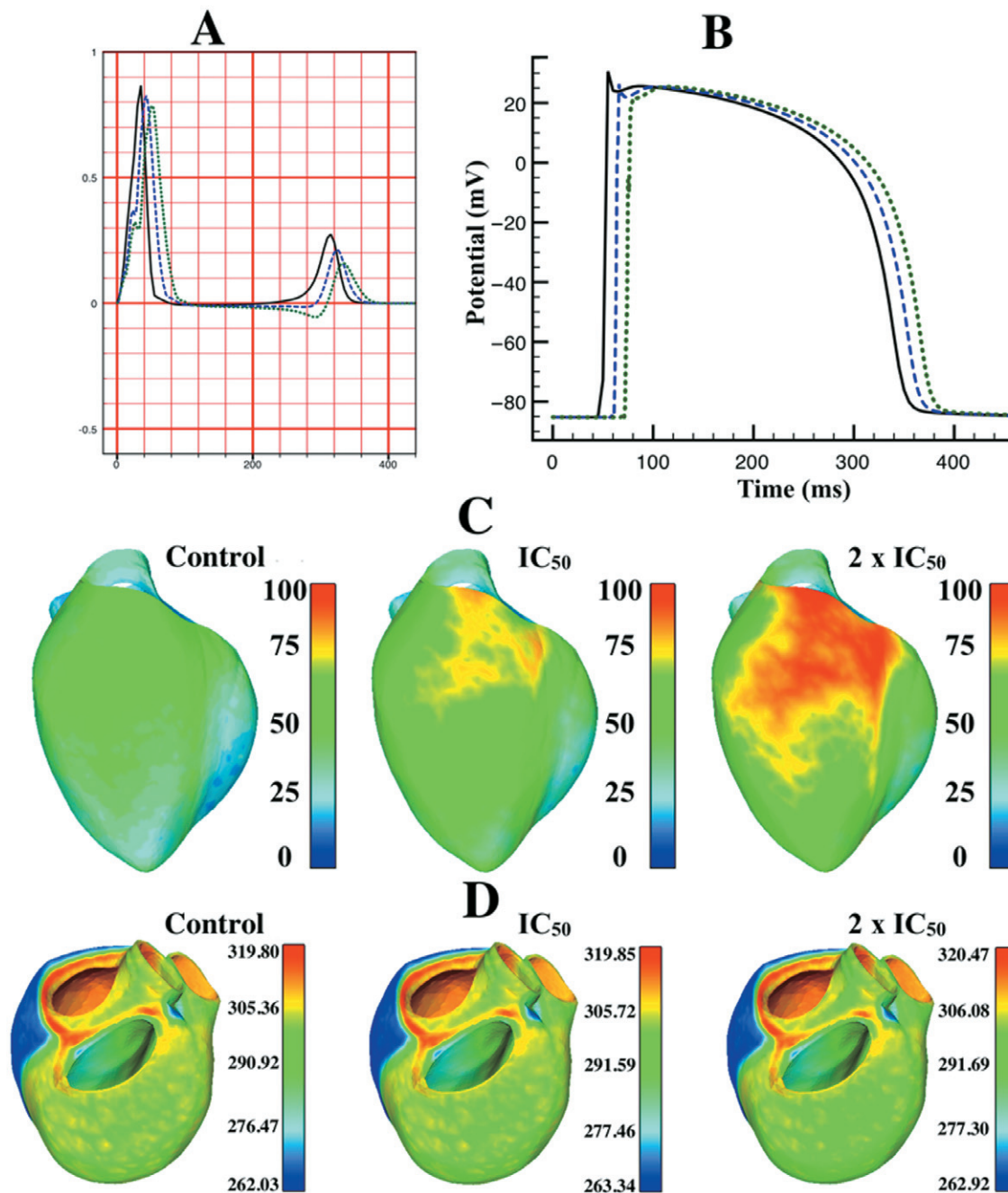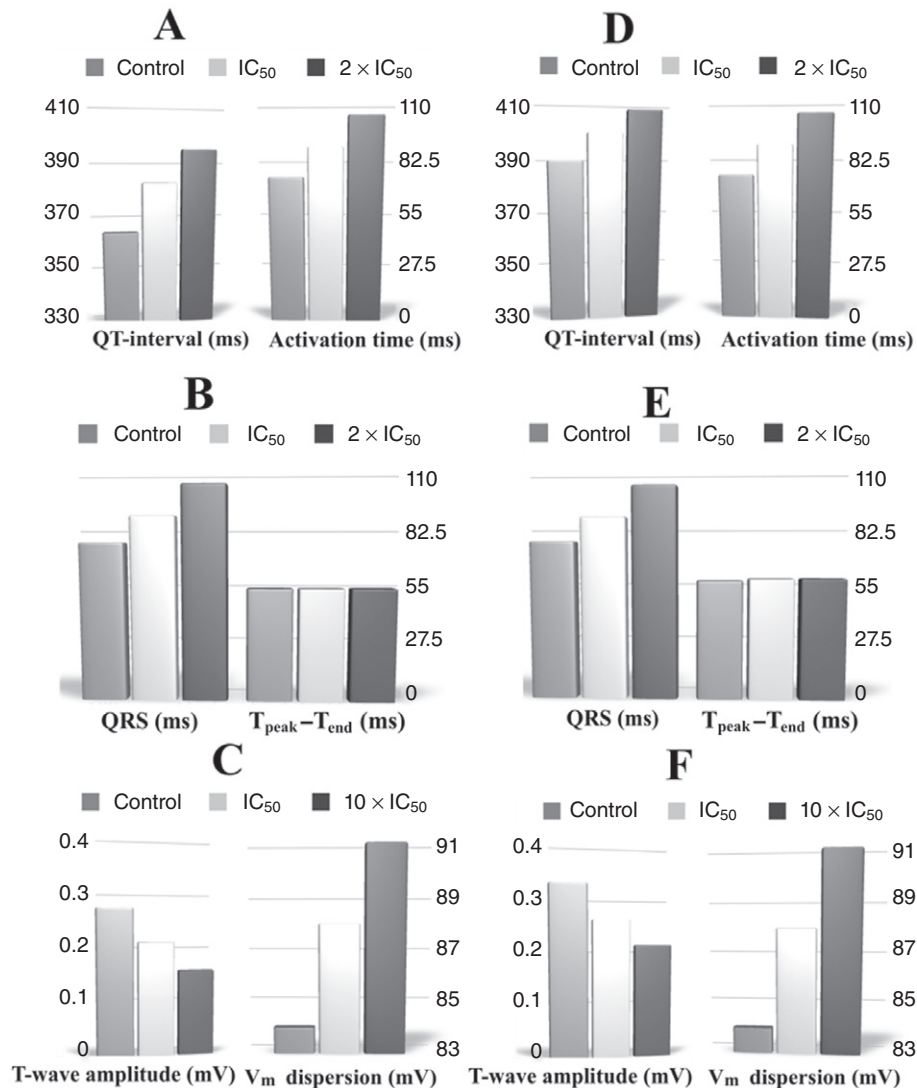
Figure 8

Simulated effect of sodium channel block on the body surface ECG (A), the action potential (B), activation maps (C, left ventricle wall view) and APD$_{90}$ maps (D, basal view) for normal conditions, IC$_{50}$ dose and 10 times the IC$_{50}$ dose. Times are in ms. (A) X-axis (small square, 40 ms; big square, 200 ms), Y-axis (small square, 0.1 mV; big square, 0.5 mV).

to evaluate the ability of our model to reproduce known effects. However, simulations using our model could be conducted for drugs acting simultaneously on multiple channels, using the known IC$_{50}$ values for each of the channels (similar to the studies by Davies *et al.*, 2012; Mirams *et al.*, 2011). Examples of such drugs include, e.g., Pimozide, which is a class II drug with IC$_{50}$ values for sodium and hERG channels of 54 and 20 nM respectively (see Redfern *et al.*, 2003; Mirams

et al., 2011). This drug and other antipsychotic drugs increase the arrhythmic risk (Mackin, 2008). Another example is Quinidine, a class I drug, used to treat atrial and ventricular fibrillation, but with pro-arrhythmic potential (Yang and Roden, 1996). Quinidine has been shown to block components of the sodium current, as well as the calcium and potassium, with hERG IC$_{50}$ value 50 times lower than its sodium IC$_{50}$ (Redfern *et al.*, 2003; Mirams *et al.*, 2011).

Figure 9

Histograms comparing the effect of a sodium blocker on the biomarkers for control condition IC_{50} dose and two times IC_{50}dose, when the L-type calcium current level is 100% (A, B and C) and when L-type calcium current level is 130% (D, E and F). Panel A (resp. D) compares the QT-interval and activation time for the three drug doses when the L-type calcium current level is 100% (resp. 130%). Panel B (resp. E) compares the QRS duration and the T_{peak}–T_{end} when the L-type calcium current level is 100% (resp. 130%). Panel C (resp. F) compares T-wave amplitude and AP dispersion when the L-type calcium current level is 100% (resp. 130%).

In addition to the simulation of multi-channel drug effects, our tool could also be used to predict multi-drug action on the ventricles, as the risk of toxicity is higher when using multiple drugs (Thummel and Wilkinson, 1998). Our study shows that modelling and simulating multiple drug administration could be addressed for suspect combination of drugs.

In general, the simulated ECGs are promising, since the global ECG features could be clearly seen in the simulated signals. Nevertheless, there are many details to improve in order to reproduce an accurate representation of the ECGs: In particular, the QRS complex and the T-wave amplitude in the limb and augmented leads should be improved. As concerns the T-wave amplitude, the cell heterogeneity is a key of the problem. There is still a debate between the fact the trans-

mural and/or apico-basal heterogeneity is modulating the T-wave polarity and amplitude. In this work, we made the choice to use only transmural heterogeneity. This seems to not be enough in order to generate a sufficiently physiological T wave.

Conclusions and perspectives

In this paper, we presented a computational simulation showing the effect of specific drug doses on the ECG measured on the thorax surface. A combination of state-of-the-art modelling and simulation tools and methodologies are used in this work, which include a finite element mesh of the human body, a biophysically detailed human bidomain

model of cardiac electrophysiological activity, a model of drug/ion channel interactions and an efficient open source software package.

Simulation results are presented showing how increasing ion channel block (or increasing the drug dose) alters the action potential, ventricular activation and repolarization and the ECG. Potassium current (or hERG) block results in prolongation of the QT interval due to APD prolongation, which has been related to increased risk of Torsades de Pointes. Block of the fast sodium current causes prolongation of the QRS interval, a known cardiac risk marker, especially for class 1C anti-arrhythmic drugs. These results are in accordance with the clinical findings on the effect of sodium and potassium ion channel blockers on the electrophysiology of the heart, and in particular on their effect on the QT interval of the ECG. We also assessed the effect of increasing the L-type calcium in the modulation of drug effects on the ECG.

We consider that the ECG simulator could be used as a tool for the prediction of drug effects on the QT interval and other ECG-based biomarkers for drug safety testing. It could also be used for insight into and more understanding of the drug mechanism at the organ level resulting from the complex interplay between cardiac structure and nonlinear membrane kinetics.

We believe that assessing the effect of single channel block on the electrical activity of the heart from the cell level to the ECG level is an important step before assessing multiple channel effects. This allows distinguishing each of the possible channel block effects on the APD and ECG. In future studies, we will consider multichannel drug effects by using the different IC_{50} values of the drug with respect to their corresponding ion channels as obtained from ion channel assays.

The models and simulations presented here constitute a significant step forward towards realistic simulation of drug-induced effects on the ECG.

Although the TP06 cell model provides a description of calcium handling, the formulation is still a simplification and cannot describe all details of calcium dynamics. Future work will aim at overcoming some of the limitations of our current model by, for example, including a physiological model representing the physiological details of the calcium dynamic, the representation of important cardiac structures such as the specialized conduction system as previously done in (Bordas et al., 2011) for rabbit, as well as a more systematic investigation on the role of electrophysiological heterogeneities in determining drug effects on the heart. These state-of-the-art methodologies could be a useful tool in the assessment of drug cardiotoxicity and can also be extended to the investigation of the effect of mutations or disease on the ECG.

Acknowledgements

Conflict of interest

None.

References

Abi-Gerges N, Philp K, Pollard C, Wakefield I, Hammond TG, Valentin JP (2004). Sex differences in ventricular repolarization: from cardiac electrophysiology to Torsades de Pointes. Fundam Clin Pharmacol 18: 139–151.

Adams CP, Brantner VV (2006). Estimating the cost of new drug development: is it really $802 million? Health Aff 25: 420–428.

Aehlert B (2006). Ecgs Made Easy. third edn. Elsevier: Mosby Jems.

Bernabeu MO, Bishop MJ, Pitt-Francis J, Gavaghan DJ, Grau V, Rodriguez B (2008). High performance computer study of biological function in 3D heart models incorporating fibre orientation and realistic geometry at para-cellular resolution. Comput Cardiol 2008: 721–724.

Bezzina CR, Shimizu W, Yang P, Koopmann TT, Tanck MWT, Miyamoto Y et al. (2006). Common sodium channel promoter haplotype in asian subjects underlies variability in cardiac conduction. Circulation 113: 338–344.

Bishop MJ, Hales P, Plank G, Gavaghan DJ, Scheider J, Grau V (2009). Comparison of rule-based and DTMRI-derived fibre architecture in a whole rat ventricular computational model. Lect Notes Comput Sci 5528: 87–96.

Bordas R, Gillow K, Lou Q, Efimov I, Kohl P, Gavaghan D et al. (2011). Full rabbit-specific ventricular model of cardiac electrophysiological function including specialized conduction system. Prog Biophys Mol Biol 107: 90–100.

Boulakia M, Cazeau S, Fernandez MA, Gerbeau JF, Zemzemi N (2010). Mathematical modeling of electrocardiograms: a numerical study. Ann Biomed Eng 38: 1071–1097.

Brennan T, Fink M, Rodriguez B (2009). Multiscale modelling of drug-induced effects on cardiac electrophysiological activity. Eur J Pharm Sci 36: 62–77.

Chapelle D, Fernndez MA, Gerbeau JF, Moireau P, Sainte-Marie J, Zemzemi N (2009). Numerical simulation of the electromechanical activity of the heart. In: Ayache N, Delingette H, Sermesant M (eds). Functional Imaging and Modeling of the Heart, Volume 5528 of Lecture Notes in Computer Science. Springer: Berlin, pp. 357–365.

Clancy CE, Rudy Y (1999). Linking a genetic defect to its cellular phenotype in a cardiac arrhythmia. Nature 400: 566–569.

Clancy CE, Rudy Y (2001). Cellular consequences of herg mutations in the long qt syndrome: precursors to sudden cardiac death. Cardiovasc Res 50: 301–313.

Clements J, Nenonen J, Li PKJ, Horacek BM (2004). Activation dynamics in anisotropic cardiac tissue via decoupling. Ann Biomed Eng 2: 984–990.

Clerc L (1976). Directional differences of impulse spread in trabecular muscle from mammalian heart. J Physiol 255: 335–346.

Cooper J (2009). Automatic Validation and Optimisation of Biological Models. *DPhil Thesis, University of Oxford.*

Corrias A, Jie X, Romero L, Bishop MJ, Bernabeu M, Pueyo E *et al.* (2010). Arrhythmic risk biomarkers for the assessment of drug cardiotoxicity: from experiments to computer simulations. Philos Trans R Soc A 368: 3001–3025.

Curran ME, Splawski I, Timothy KW, Vincent GM, Green DE, Keating MT (1995). A molecular basis for cardiac arrhythmia: herg mutations cause long qt syndrome. Cell 80: 795–803.

Davies MR, Mistry HB, Hussein L, Pollard CE, Valentin J-P, Swinton J *et al.* (2012). An In silico canine cardiac midmyocardial action potential duration model as a tool for early drug safety assessment. Am J Physiol Heart Circ Physiol 302: 466–480.

De Bruin ML, Pettersson M, Meyboom RHB, Hoes AW, Leufkens HGM (2005). Anti-herg activity and the risk of drug-induced arrhythmias and sudden death. Eur Heart J 26: 590–597.

Dux-Santoy L, Sebastian R, Felix-Rodriguez J, Ferrero J, Saiz J (2011). Interaction of specialized cardiac conduction system with antiarrhythmic drugs: a simulation study. IEEE Trans Biomed Eng 58: 3475–3478.

Epstein BR, Foster KR (1983). Anisotropy in the dielectric properties of skeletal muscle. Med Biol Eng Comput 21: 51–55.

Fletcher K, Shah RR, Thomas A, Tobin F, Rodriguez B, Mirams G (2011). Novel approaches to assessing cardiac safety-proceedings of a workshop: regulators, industry and academia discuss the future of in silico cardiac modelling to predict the proarrhythmic safety of drugs. Drug Saf 34: 439–443.

Fossa AA, DePasquale MJ, Raunig DL, Avery MJ, Leishman DJ (2002). The relationship of clinical qt prolongation to outcome in the conscious dog using a beat-to-beat qt-rr interval assessment. J Pharmacol Exp Ther 302: 828–833.

Frey P (2001). Yams: a fully automatic adaptive isotropic surface remeshing procedure. Technical report 0252, INRIA-Rocquencourt, France.

George PL, Hecht F, Saltel E (1990). Fully automatic mesh generator for 3d domains of any shape. Impact Comput Sci And Eng 2: 187–218.

Gima K, Rudy Y (2002). Ionic current basis of electrocardiographic waveforms: a model study. Circ Res 90: 889.

Gintant G (2011). An evaluation of herg current assay performance: translating preclinical safety studies to clinical qt prolongation. Pharmacol Ther 129: 109–119.

Glukhov AV, Fedorov VV, Lou Q, Ravikumar VK, Kalish PW, Schuessler RB *et al.* (2010). Transmural dispersion of repolarization in failing and nonfailing human ventricle. Circ Res 106: 981–991.

Grandy SA, Howlett SE (2006). Cardiac excitation-contraction coupling is altered in myocytes from aged male mice but not in cells from aged female mice. Am J Physiol Heart Circ Physiol 291: H2362–H2370.

Hancox JC, McPate MJ, El Harchi A, Zhang Y (2008). The herg potassium channel and herg screening for drug-induced torsades de pointes. Pharmacol Ther 119: 118–132.

Hondeghem M, Carlsson M, Duker G (2001). Instability and triangulation of the action potential predict serious proarrhythmia, but action potential duration prolongation is antiarrhythmic. Circulation 103: 2004–2013.

ICH. E14 (2005). The clinical evaluation of qt/qtc interval prolongation and proarrhythmic potential for non-anti arrhythmic drugs. Technical report.

Janse MJ, Coronel R, Opthof T, Sosunov EA, Anyukhovsky EP, Rosen MR (2012). Repolarization gradients in the intact heart: transmural or apico-basal? Prog Biophys Mol Biol 109: 6–15.

Karjalainen J, Viitasalo M, Manttari M, Manninen V (1994). Relation between qt intervals and heart rates from 40 to 120 beats/min in rest electrocardiograms of men and a simple method to adjust qt interval values. J Am Coll Cardiol 23: 1547–1553.

Keller DUJ, Weiss DL, Doessel O, Seemann G (2011). Influence of IKs Heterogeneities on the Genesis of the T-Wave: a computational evaluation. IEEE Trans Biomed Eng 99: 1–1.

Kohlhardt M, Bauer B, Krause H, Fleckenstein A (1972). Differentiation of the transmembrane na and ca channels in mammalian cardiac fibres by the use of specific inhibitors. Pflugers Arch 335: 309–322.

Kowey PR, Malik M (2007). The qt interval as it relates to the safety of non-cardiac drugs. Eur Heart J Suppl 9 (Suppl. G): G3.

Krikler DM, Curry PV (1976). Torsade de pointes, an atypical ventricular tachycardia. Br Heart J 38: 117–120.

Lines GT, Buist ML, Grottum P, Pullan AJ, Sundnes J, Tveito A (2003a). Mathematical models and numerical methods for the forward problem in cardiac electrophysiology. Comput Vis Sci 5: 215–239.

Lines GT, Grottum P, Tveito A (2003b). Modeling the electrical activity of the heart: a bidomain model of the ventricles embedded in a torso. Comput Vis Sci 5: 195–213.

Lu HR, Vlaminckx E, Hermans AN, Rohrbacher J, Van Ammel K, Towart R *et al.* (2008). Predicting drug-induced changes in QT interval and arrhythmias: QT-shortening drugs point to gaps in the ICHS7B Guidelines. Br J Pharmacol 154: 1427–1438.

Lu HR, Rohrbacher J, Vlaminckx E, Ammel KV, Yan G-X, Gallacher DJ (2010). Predicting drug-induced slowing of conduction and pro-arrhythmia: identifying the 'bad' sodium current blockers. BJP 160: 60–76.

Mackin P (2008). Cardiac side effects of psychiatric drugs. Hum Psychopharmacol 23: S3–S14.

Malik M, Farbom P, Batchvarov V, Hnatkova K, Camm AJ (2002). Relation between qt and rr intervals is highly individual among healthy subjects: implications for heart rate correction of the qt interval. Heart 87: 220–228.

Malmivuo J, Plonsey R (1995). Bioelectromagnetism. Principles and Applications of Bioelectric and Biomagnetic fields. Oxford University Press: New York.

Mirams GR, Cui Y, Sher A, Fink M, Cooper J, Heath BM *et al.* (2011). Simulation of multiple ion channel block provides improved early prediction of compounds clinical torsadogenic risk. Cardiovasc Res 91: 53–61.

Miura M, Ishide N, Oda H, Sakurai M, Shinozaki T, Takishima T (1993). Spatial features of calcium transients during early and delayed afterdepolarizations. Am J Physiol Heart Circ Physiol 265: 439–444.

Moreno JD, Zhu Zi, Wang PC, Bankston JR, Jeng MT, Kang C *et al.* (2011). A computational model predict the effects of class I anti-arrhythmic drugs on venticular rhythms. Sci Transl Med 3: 83–98

Niederer SA, Kerfoot E, Benson AP, Bernabeu MO, Bernus O, Bradley C *et al.* (2011). Verification of cardiac tissue

electrophysiology simulators using an n-version benchmark. Philosophical Transactions of the Royal Society A: mathematical. Phys Eng Sci 369: 4331–4351.

Noble D (2008). Computational models of the heart and their use in assessing the actions of drugs. J Pharmacol Sci 107: 107–117.

Pathmanathan P, Bernabeu MO, Bordas R, Cooper J, Garny A, Pitt-Francis J et al. (2010). A numerical guide to the solution of the bidomain equations of cardiac electrophysiology. Prog Biophys Mol Biol 102: 136–155.

Pitt-Francis J, Pathmanathan P, Bernabeu MO, Bordas R, Cooper J, Fletcher AG et al. (2009). Chaste: a test-driven approach to software development for biological modelling. Comput Phys Commun 180: 2452–2471.

Pollard CE, Abi Gerges N, Bridgland-Taylor MH, Easter A, Hammond TG, Valentin J et al. (2010). An introduction to qt interval prolongation and non-clinical approaches to assessing and reducing risk. Br J Pharmacol 159: 12–21.

Potse M, Dube B, Gulrajani M (2003). ECG simulations with realistic human membrane, heart, and torso models. In Proceedings of the 25th Annual International Conference of the IEEE EMBS, pages 70–77.

Potse M, Dube B, Vinet A (2009). Cardiac anisotropy in boundary-element models for the electrocardiogram. Med Biol Eng Comput 47: 719–729.

Pueyo E, Husti Z, Hornyik T, Baczko I, Laguna P, Varro A et al. (2010). Mechanisms of ventricular rate adaptation as a predictor of arrhythmic risk. Am J Physiol Heart Circ Physiol 298: H1577–HI587.

Pugsley MK, Authier S, Curtis MJ (2008). Principles of safety pharmacology. Br J Pharmacol 154: 1382–1399.

Pullan AJ, Buist ML, Cheng LK (2005). Mathematically Modelling the Electrical Activity of the Heart. From Cell to Body Surface and Back Again. World Scientific Publishing Co. Pte. Ltd.: Singapore.

Recanatini M, Poluzzi E, Masetti M, Cavalli A, De Ponti F (2005). Qt prolongation through herg k+ channel blockade: current knowledge and strategies for the early prediction during drug development. Med Res Rev 25: 133–166.

Redfern WS, Carlsson L, Davis AS, Lynch WG, MacKenzie I, Palethorpe S et al. (2003). Relationships between preclinical cardiac electrophysiology, clinical qt interval prolongation and torsade de pointes for a broad range of drugs: evidence for a provisional safety margin in drug development. Cardiovasc Res 58: 32–45.

Romero L, Pueyo E, Fink M, Rodriguez B (2009). Impact of ionic current variability on human ventricular cellular electrophysiology. Am J Physiol Heart Circ Physiol 297: 14–36.

Rush S, Driscoll DA (1969). Eeg electrode sensitivity-an application of reciprocity. IEEE Trans Biomed Eng 1: 15–22.

Saiz J, Tena G, Monserrat M, Ferrero JM, Cardona K, Chorro J (2011). Effects of the antiarrhythmic drug dofetilide on transmural dispersion of repolarization in ventriculum. A computer modeling study. IEEE Trans Biomed Eng 58: 43–53.

Salata JJ, Wasserstrom JA (1988). Effects of quinidine on action potentials and ionic currents in isolated canine ventricular myocytes. Circ Res 62: 324–337.

Sale H, Wang J, O'Hara TJ, Tester DJ, Phartiyal P, He JQ et al. (2008). Physiological properties of hERG 1a/1b heteromeric currents and a hERG 1b-specific mutation associated with long-QT syndrome. Circ Res 103: 81–95.

Sanchez C, Corrias A, Bueno-Orovio A, Davies M, Swinton J, Jacobson I et al. (2012). The Na+/K+ pump is an important modulator of refractoriness and rotor dynamics in human atrial tissue. AJP 302: 146–159.

Sanguinetti MC, Mitcheson JS (2005). Predicting drug-herg channel interactions that cause acquired long qt syndrome. Trends Pharmacol Sci 26: 119–124.

Schwan HP, Kay CF (1957). The conductivity of living tissues. Ann N Y Acad Sci 65: 1007–1013.

Shimizu W, Antzelevitch C (1997). Sodium channel block with mexiletine is effective in reducing dispersion of repolarization and preventing torsade de pointes in lqt2 and lqt3 models of the long-qt syndrome. Circulation 96: 2038–2047.

Sims C, Reisenweber S, Viswanathan PC, Choi BR, Walker WH, Salama G (2008). Sex, age, and regional differences in l-type calcium current are important determinants of arrhythmia phenotype in rabbit hearts with drug-induced long qt type 2. Circ Res 102: 86–100.

Soubert A, Helmlinger G, Dumotier B, Bibas R, Georgieva A (2009). Modeling and simulation of preclinical cardiac safety: towards an integrative framework. Drug Metab Pharmacokinet 24: 76–90.

Straus SMJM, Sturkenboom MCJM, Bleumink GS, Dieleman JP, Lei J, Graeff PA et al. (2005). Non-cardiac qtc-prolonging drugs and the risk of sudden cardiac death. Eur Heart J 26: 2007–2012.

Sundnes J, Lines GT, Cai X, Nielsen BF, Mardal KA, Tveito A (2006). Computing the Electrical Activity in the Heart. Springer-Verlag: Berlin Heidelberg, New York.

Ten Tusscher K, Panfilov AV (2006). Cell model for effcient simulation of wave propagation in human ventricular tissue under normal and pathological conditions. Phys Med Biol 51: 6141–6156.

Thummel KE, Wilkinson GR (1998). In vitro and in vivo drug interactions involving human cyp3a. Annu Rev Pharmacol Toxicol 38: 389–430.

Tung L (1978). A bi-domain model for describing ischemic myocardial D–C potentials. PhD thesis, MIT.

Valentin JP, Hammond T (2008). Safety and secondary pharmacology: successes, threats, challenges and opportunities. J Pharmacol Toxicol Methods 58: 77–87.

Valentin JP, Hoffmann P, De Clerck F, Hammond TG, Hondeghem LM (2004). Review of the predictive value of the langendorff heart model (screenit system) in assessing the proarrhythmic potential of drugs. J Pharmacol Toxicol Methods 49: 171–181.

Vandenberg JI, Walker BD, Campbell TJ (2001). Herg k+ channels: friend and foe. Trends Pharmacol Sci 22: 240–246.

Verkerk AO, Wilders R, Veldkamp MW, Geringel W, Kirkels JH, Tan HL (2005). Gender disparities in cardiac cellular electrophysiology and arrhythmia susceptibility in human failing ventricular myocytes. Int Heart J 46: 1105–1118.

Volders PGA, Vos MA, Szabo B, Sipido KR, De Groot SH, Gorgels APM et al. (2000). Progress in the understanding of cardiac early afterdepolarizations and torsades de pointes: time to revise current concepts. Cardiovasc Res 46: 376–392.

Yan GX, Lankipalli RS, Burke JF, Musco S, Kowey PR (2003). Ventricular repolarization components on the electrocardiogram: cellular basis and clinical significance. J Am Coll Cardiol 42: 401–409.

Yang T, Roden MD (1996). Extracellular potassium modulation of drug block of ikr: implications for torsade de pointes and reverse use dependence. Circulation 93: 407–411.

Yap YG, Camm AJ (2003). Drug induced QT prolongation and torsades de pointes. BMJ 89: 1363–1372.

Zemzemi N (2009). Etude theorique et numerique de l'activite electrique du Coeur: application aux electrocardiogrammes. *DPhil Thesis. University of Paris-Sud, Paris-IX*. Available at: http://tel.archives-ouvertes.fr/tel-00470375/en/ (accessed 14 December 2009).

Zemzemi N, Bernabeu MO, Saiz J, Rodriguez B (2011). LCNS. Springer-Verlag: Berlin-Heidelberg.

Supporting information

Additional Supporting Information may be found in the online version of this article:

Appendix S1 Mathematical ECG and drug models.